cleavage is fully rate-limiting. Thus, the structure of the transition state for this decarboxylation does not change significantly under these three conditions. The results confirm the hypothesis that desolvation by a protein binding pocket or by organic solvents can cause a very large acceleration in the rate of a decarboxylation reaction but does not significantly alter the transition-state structure as reflected by the carbon isotope effect.

Acknowledgment. This research is supported in part by Faculty Research Award FRA369 from the American Cancer Society, Grant No. GM38273 from the National Institutes of Health, the Alfred P. Sloan Foundation (D.H.), grant GM43043 from the National Institutes of Health (M.H.O.), and a fellowship from the Jane Coffin Childs Memorial Fund for Medical Research (C.L.).

Voltammetric Characterization of Rapid and Reversible Binding of an Exogenous Thiolate Ligand at a [4Fe-4S] Cluster in Ferredoxin III from *Desulfovibrio africanus*

Julea N. Butt, Artur Sucheta, Fraser A. Armstrong,* Jacques Breton,† Andrew J. Thomson,† and E. Claude Hatchikian‡

Contribution from the Department of Chemistry, University of California, Irvine, California 92717, School of Chemical Sciences, University of East Anglia, Norwich NR4 7TJ, U.K., and Laboratoire de Chimie Bacterienne, CNRS, PB 71, 13277 Marseille, France. *Received June 19, 1992*

Abstract: Rapid and reversible, redox-coupled binding of an exogenous ligand to an Fe-S cluster in a protein has been studied by voltammetry. Ferredoxin III from *Desulfovibrio africanus* contains a [3Fe-4S] cluster whose transformation into a [4Fe-4S] center generates a new site for coordination. By coadsorbing with neomycin or polymyxin, an electroactive film of the protein is obtained at an edge-oriented pyrolytic graphite electrode which is then introduced to solutions containing the ligand. The equilibria and kinetics of ligation are determined by inspection and digital simulation of voltammograms measured over a range of scan rates. For solutions of 2-mercaptoethanol, results are consistent with coordination of the thiolate anion at both oxidized (dissociation constant = 28 μM) and reduced (dissociation constant = 97 mM) forms of the transformed [4Fe-4S] cluster. Direct detection of the thiolate-ligated reduced cluster by EPR is not feasible because the high concentration of mercaptoethanol that is required in solution results in cluster degradation. No interaction with thiolate is detected for the indigenous, stable [4Fe-4S] cluster or for the untransformed [3Fe-4S] precursor cluster. Under fast-scan conditions, the thiolate-ligated species appears as a trapped redox couple with $E^{\circ\prime}$ = -585 mV (cf. -396 mV for the native species) whereas, at a slow scan rate, equilibrium is established at all times and the observed reduction potential of the new couple depends upon thiolate concentration. At intermediate scan rates, a combination of trapped and dynamic, equilibrating species is observed. The great disparity in the equilibrium constants, reflected in the marked change in reduction potential, is attributed to a much faster rate of thiolate coordination to the *oxidized* cluster. An associative mechanism is proposed, involving nucleophilic attack by thiolate at the labile Fe subsite. The experiment provides a simple yet profound demonstration of time-separated coupling between electron transfer and ligand exchange (more generally extendable to conformational change) in a metalloprotein.

Introduction

Interest in Fe-S clusters has taken a new and unexpected direction with the realization that they have roles other than electron transfer.[1,2] They are now known to occur in several (de)hydratases,[3-6] the most thoroughly characterized of which is mitochondrial aconitase.[1,4-6] In its active form, aconitase contains a [4Fe-4S] cluster, one Fe of which is coordinated not to cysteine but to a hydroxide ion.[4,5] This 'subsite-differentiated' Fe is a Lewis acid catalyst, binding substrates (citrate, aconitate, isocitrate) and inhibitors,[5,6] but during aerobic isolation, it is released, resulting in formation of an inactive enzyme containing a [3Fe-4S] cluster.[1] The enzyme is reactivated by addition of Fe(II) under reducing conditions. A similar type of redox-linked [3Fe-4S] ↔ [4Fe-4S] transformation is known to occur for many other Fe-S proteins.[7-9] Moreover, metals other than Fe can readily be added to form heterometal [M3Fe-4S] clusters.[10-13] An important further development has occurred with characterization of the iron responsive element-binding protein (IRE-BP), a protein whose ability to bind to iron responsive elements (IRE's) located in mRNA is dependent upon the Fe status of the cell.[14] The discovery[15] that IRE-BP has close sequence homology with aconitase has suggested

Scheme I

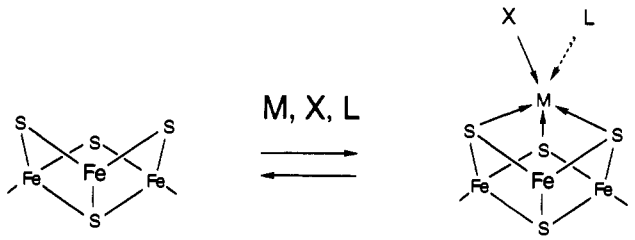

that the Fe sensory mechanism is linked to some difference in the properties of [3Fe-4S] and [4Fe-4S] forms.[54] It has furthermore

* Author to whom correspondence should be addressed at the University of California.
† University of East Anglia.
‡ Laboratoire de Chimie Bacterienne.

(1) Beinert, H.; Kennedy, M. C. *Eur. J. Biochem.* **1989**, *186*, 5. Emptage, M. H. In *Metal Clusters in Proteins*; Que, L., Ed.; ACS Symposium Series 372; American Chemical Society; Washington, DC, 1988; p 343.
(2) Switzer, R. L. *Biofactors* **1989**, *2*, 77. Beinert, H. *FASEB J.* **1990**, *4*, 2483. Cammack, R. In *Advances in Inorganic Chemistry*; Sykes, A. G., Cammack, R., Eds.; Academic Press: New York, 1992; p 281.
(3) Grabowski, R.; Buckel, W. *Eur. J. Biochem.* **1991**, *199*, 89. Flint, D. H.; Emptage, M. H.; Guest, J, R. *Biochemistry* **1992**, *31*, 10331. Flint, D. H.; Emptage, M. H. *J. Biol. Chem.* **1988**, *263*, 3558. Kuchta, R. D.; Hanson, G. R.; Holmquist, B.; Abeles, R. H. *Biochemistry* **1986**, *25*, 7301. Kelly, J. M.; Scopes, R. K. *FEBS Lett.* **1986**, *202*, 274. Dreyer, J.-L. *Eur. J. Biochem.* **1985**, *150*, 145. Scopes, R. K.; Griffiths-Smith, K. *Anal. Biochem.* **1984**, *136*, 530. Schweiger, G.; Dutscho, R.; Buckel, W. *Eur. J. Biochem.* **1987**, *169*, 441.

0002-7863/93/1515-1413$04.00/0

been reported that IRE-BP is identical to a cytosolic form of aconitase.[16] A more general hypothesis, that a function of certain ferredoxins may be to interact with DNA in a manner depending upon cluster status, has recently been proposed.[17] Iron–sulfur clusters have indeed been found in certain DNA repair enzymes,[18] and there is even evidence for their presence in a transcription factor.[19] The role of the clusters in these and other proteins[20] remains unclear, but a close involvement with control or stabilization of the protein conformation is again likely. Relevant to this is the observation made by Burgess and co-workers,[21] that if one of the cysteine ligands normally coordinating the [4Fe–4S] cluster in ferredoxin I (*Azotobacter vinelandii*) is substituted by site-directed mutagenesis, the cluster recruits an alternative ligand, thus enforcing a change in the conformation of the protein.

Thus, by contrast with the long-held notion of clusters as inert electron-transfer centers, these developments reveal functional diversity and suggest a propensity for *communication*, i.e. an ability in certain cases to exchange metal ions and ligands (in the case of aconitase, a transformable substrate) with the environment. From Scheme I, two levels of action are immediately identified. First, by its intrinsic ability to coordinate a fourth metal ion M, the [3Fe–4S] cluster must be regarded as a ligand.[12,13,22] Second, the addition of M to a [3Fe–4S] core creates a new center for coordination of donor groups that may be provided by various protein side chains X and/or exogenous ligands L. Such a cluster now constitutes an 'engine' for conformational change—one that is activated by a specific metal ion or metal ion/ligand combination. Since the [M3Fe–4S] cluster can exist in more than one oxidation level, these reactions will be linked to the environmentally-imposed electrochemical potential and may be dynamically coupled to electron transport.

It is thus important to identify reactivity trends and determine whether there are rules, widely applicable among proteins, that govern the equilibria and kinetics of these types of reactions. Questions to be addressed include the comparative reactivities of various metals M and ligands L and the influence of cluster oxidation level on rates and equilibria. While the facility with which ligand exchange can occur at Fe–S clusters has long been recognized and indeed exploited,[23-27] the quantitative aspects remain unclear. The clearest, general mechanistic picture of ligand exchange at Fe–S clusters has stemmed from studies of synthetic analogue complexes in aprotic solvents. Holm and co-workers investigated[26] thiolate substitution reactions of the tetrakis(alkanethiolate) (RS^-) analogue complexes $[Fe_4S_4(SR)_4]^{2-}$ in acetonitrile. They noted that rates of replacement of RS^- by various arenethiolates $R'S^-$ increased with increasing arenethiol acidity or in the presence of added acetic or benzoic acid. In studies[27] of the reaction of $[Fe_4S_4(SPh)_4]^{2-/3-}$ with the electrophile acetic anhydride, in which PhS^- is replaced by acetate, it was found that the exchange process proceeded more rapidly with the reduced cluster. Each of these observations supports a mechanism in which the rate-determining step is electrophilic attack by HA (acid catalyst) or R'SH on the bound RS^-. For aqueous solutions, however, a feasible alternative is that the controlling factor is *nucleophilic* attack at an Fe subsite by the incoming ligand. This is indeed evident from the studies of Job and Bruice[25] with the water-soluble analogue $[Fe_4S_4(SCH_2CH_2CO_2^-)_4]^{6-}$.

More recently, Holm's group has synthesized site-specific [4Fe–4S] analogues[28,29] in which three of the four Fe subsites are ligated by a tridentate trithiolate ligand while the fourth Fe has an exchangeable ligand such as chloride. Products arising from regiospecific ligand substitution at the unique subsite have been characterized by NMR and electrochemistry. Ligand substitution by monodentate, bidentate, and tridentate ligands gives products[28] in which the unique Fe subsite is respectively four-, five-, and six-coordinate. These give chemically reversible cyclic voltammetry in dichloromethane solution. The greater [4Fe–4S] core electron density afforded by increasing the number of donor groups at this unique Fe subsite results in a substantial negative shift in the reduction potential of the 2+/1+ (and 3+/2+) couples.

In proteins, such ligand-exchange reactivity may be more common than is generally realized. In addition to the rapid coordination of substrates at the cluster in active aconitase, the $[4Fe–4S]^{1+}$ cluster of *Pyrococcus furiosus* ferredoxin (which also has one non-cysteine ligand[9,30]) has been shown by EPR spectroscopy to coordinate CN^- when incubated in concentrated solutions of this ligand.[31] In recent publications,[8,12,13] we have described studies of rapid and reversible reactions of various metal ions (Fe(II), Zn(II), Cd(II), and Tl(I)) with a [3Fe–4S] cluster in a protein. The subject of these studies was ferredoxin III (Fd III) from *Desulfovibrio africanus* (MW 6600). This protein has seven cysteines, four of which ligate a [4Fe–4S] cluster in the typical manner, with the remaining three cysteines ligating the transformable [3Fe–4S] cluster.[32,33] Our studies have exploited

(4) Robbins, A. H.; Stout, C. D. *Proc. Natl. Acad. Sci. U.S.A.* **1989**, *86*, 3639.
(5) Werst, M. M.; Kennedy, M. C.; Beinert, H.; Hoffman, B. M. *Biochemistry* **1990**, *29*, 10526.
(6) Lauble, H.; Kennedy, M. C.; Beinert, H.; Stout, C. D. *Biochemistry* **1992**, *31*, 2735.
(7) Moura, J. J. G.; Moura, I.; Kent, T. A.; Lipscomb, J. D.; Huynh, B.-H.; LeGall, J.; Xavier, A. V.; Münck, E. *J. Biol. Chem.* **1982**, *257*, 6259.
(8) George, S. J.; Armstrong, F. A.; Hatchikian, C. C.; Thomson, A. J. *Biochem. J.* **1989**, *264*, 275.
(9) Conover, R. C.; Kowal, A. T.; Fu, W.; Park, J.-B.; Aono, S.; Adams, M. W. W.; Johnson, M. K. *J. Biol. Chem.* **1990**, *265*, 8533.
(10) Moura, I.; Moura, J. J. G.; Münck, E.; Papaefthymiou, V.; LeGall, J. *J. Am. Chem. Soc.* **1986**, *108*, 349. Surerus, K. K.; Münck, E.; Moura, I.; Moura, J. J. G.; LeGall, J. *J. Am. Chem. Soc.* **1987**, *109*, 3805.
(11) Conover, R. C.; Park, J.-B.; Adams, M. W. W.; Johnson, M. K. *J. Am. Chem. Soc.* **1990**, *112*, 4562.
(12) Butt, J. N.; Armstrong, F. A.; Breton, J.; George, S. J.; Thomson, A. J.; Hatchikian, E. C. *J. Am. Chem. Soc.* **1991**, *113*, 6663.
(13) Butt, J. N.; Sucheta, A.; Armstrong, F. A.; Breton, J.; Thomson, A. J.; Hatchikian, E. C. *J. Am. Chem. Soc.* **1991**, *113*, 8948.
(14) Hentze, M. W.; Rouault, T. A.; Caughman, S. W.; Dancis, A.; Harford, J. B.; Klausner, R. D. *Proc. Natl. Acad. Sci. U.S.A.* **1987**, *84*, 6730. Aziz, N.; Munro, H. N. *Proc. Natl. Acad. Sci. U.S.A.* **1987**, *84*, 8478. Casey, J. C.; Hentze, M. W.; Koeller, D. M.; Caughman, S. W.; Rouault, T. A.; Klausner, R. D.; Harford, J. B. *Science* **1988**, *240*, 924. Casey, J. C.; Koeller, D. M.; Ramin, V. C.; Klausner, R. D.; Harford, J. B. *EMBO J.* **1989**, *8*, 3693. Dandekar, T.; Stripecke, R.; Gray, N. K.; Goosen, B.; Constable, A.; Johansson, H. E.; Hentze, M. W. *EMBO J.* **1991**, *10*, 1903. Constable, A.; Quick, S.; Gray, N. K.; Hentze, M. W. *Proc. Natl. Acad. Sci. U.S.A.* **1992**, *89*, 4554.
(15) Rouault, T. A.; Stout, C. D.; Kaptain, S.; Harford, J. B.; Klausner, R. D. *Cell* **1991**, *64*, 881. Hentze, M. W.; Argos, P. *Nucleic Acids Res.* **1991**, *19*, 1739. Prodromou, C.; Artymiuk, P. J.; Guest, J. R. *Eur. J. Biochem.* **1992**, *204*, 599.
(16) Kaptain, S.; Downey, W. E.; Tang, C.; Philpott, C.; Haile, D.; Orloff, D. G.; Harford, J. B.; Rouault, T. A.; Klausner, R. D. *Proc. Natl. Acad. Sci. U.S.A.* **1991**, *88*, 10109. Zheng, L.; Kennedy, M. C.; Blondin, G. A.; Beinert, H.; Zalkin, H. *Arch. Biochem. Biophys.* **1992**, *299*, 356. Kennedy, M. C.; Mende-Mueller, L.; Blondin, G. A.; Beinert, H. *Proc. Natl. Acad. Sci. U.S.A.* **1992**, *89*, 11730.
(17) Thomson, A. J. *FEBS Lett.* **1991**, *285*, 230.
(18) Cunningham, R. P.; Asahara, H.; Bank, J. F.; Scholes, C. P.; Salerno, J. C.; Surerus, K.; Münck, E.; McCracken, J.; Peisach, J.; Emptage, M. H. *Biochemistry* **1989**, *28*, 4450. Michaels, M. L.; Pham, L.; Nghiem, Y.; Cruz, C.; Miller, J. H. *Nucleic Acids Res.* **1990**, *18*, 3841.
(19) Li, P. M.; Reichert, J.; Freyd, G.; Horvitz, H. R.; Walsh, C. T. *Proc. Natl. Acad. Sci. U.S.A.* **1991**, *88*, 9210.
(20) Vollmer, S. J.; Switzer, R. L.; Debrunner, P. G. *J. Biol. Chem.* **1983**, *258*, 14284. Onate, Y. A.; Vollmer, S. J.; Switzer, R. L.; Johnson, M. K. *J. Biol. Chem.* **1989**, *264*, 18386.
(21) Martin, A.; Burgess, B. K.; Stout, C. D.; Cash, V. L.; Dean, D. R.; Jensen, G. M.; Stephens, P. J. *Proc. Natl. Acad. Sci. U.S.A.* **1990**, *87*, 598.
(22) Ciurli, S.; Holm, R. H. *Inorg. Chem.* **1991**, *30*, 743.
(23) Holm, R. H.; Ciurli, S.; Weigel, J. A. *Prog. Inorg. Chem.* **1990**, *38*, 1.
(24) Gillum, W. O.; Mortenson, L. E.; Chen, J.-S.; Holm, R. H. *J. Am. Chem. Soc.* **1977**, *99*, 584.
(25) Job, R. C.; Bruice, T. C. *Proc. Natl. Acad. Sci. U.S.A.* **1975**, *72*, 2478.
(26) Dukes, G. R.; Holm, R. H. *J. Am. Chem. Soc.* **1975**, *97*, 528.
(27) Johnson, R. W.; Holm, R. H. *J. Am. Chem. Soc.* **1978**, *100*, 5338.
(28) Ciurli, S.; Carrié, M.; Weigel, J. A.; Carney, M. J.; Stack, T. D. P.; Papaefthymiou, G. C.; Holm, R. H. *J. Am. Chem. Soc.* **1990**, *112*, 2654.
(29) Whitener, M. A.; Peng, G.; Holm, R. H. *Inorg. Chem.* **1991**, *30*, 2411. Liu, H. Y.; Scharbert, B.; Holm, R. H. *J. Am. Chem. Soc.* **1991**, *113*, 9529. Holm, R. H. In *Advanced Inorganic Chemistry*; Cammack, R., Sykes, A. G., Eds.; Academic Press: 1992; Vol. 38, p 1.
(30) Park, J.-B.; Fan, C.; Hoffman, B. M.; Adams, M. W. W. *J. Biol. Chem.* **1991**, *266*, 19351.
(31) Conover, R. C.; Park, J.-B.; Adams, M. W. W.; Johnson, M. K. *J. Am. Chem. Soc.* **1991**, *113*, 2799.
(32) Bovier-Lapierre, G.; Bruschi, M.; Bonicel, J.; Hatchikian, E. C. *Biochim. Biophys. Acta* **1987**, *913*, 20.

Table I. Redox Couples Observed for Ferredoxin III (*D. africanus*) and Derivatives in a Neomycin Film at PGE Electrodes, in Absence or Presence of Fe(II)[e]

couple	assignment	reduction potential ($E^{\circ\prime}$ vs SHE, mV)	conditions for observation	ref
A′	$[3Fe\text{–}4S]^{1+/0}$	−140[a]	7Fe form	34
B′	$[4Fe\text{–}4S]^{2+/1+}$ (stable)	−390[a]	7Fe and 8Fe forms	34
		−385[b]	8Fe form in presence of mercaptoethanol	this work
C′	$[3Fe\text{–}4S]^{0/2-}$ [c]	−720[a]	7Fe form	34
D′	$[4Fe\text{–}4S]^{2+/1+}$ (transformed from [3Fe–4S])	−393[d]	8Fe form	12
		−396[b,d]	8Fe form	this work
F′	L-$[4Fe\text{–}4S]^{2+/1+}$ (transformed from [3Fe–4S])	−585[b]	8Fe form in presence of mercaptoethanol	this work

[a] Measured at pH 7.0, 0.1 M NaCl. [b] Measured at pH 8.0–8.5, 0.2 M NaCl. [c] This is a two-electron couple, but the existence of the '2-' oxidation level has yet to be confirmed independently. [d] Couple D′ overlays couple B′; the reduction potential given is the observed average for the two couples. [e] Temperature 0 °C. Estimated errors are ±10 mV for couple A′ and ±15 mV for the couples that give broader or more complex waves.

a novel electrochemical approach[34-36] in which ferredoxin molecules are immobilized at a pyrolytic graphite surface by coadsorption with certain aminocyclitols. With such a configuration, the redox-dependent reactivities of active sites with metal ions contained in the contacting electrolyte can be monitored with considerable precision in both the time- and potential-domains. The technique is sensitive and extremely economical, requiring only minuscule amounts of protein to perform a large number of experiments. In favorable situations, it has proved possible[8,12,13] to prepare bulk samples of cluster products for spectroscopic examination and confirm that the reactivities elicited in the protein film are indeed a reflection of the properties of the protein in solution. An obvious extension of this approach is to probe the reactivities of the metal-ion-transformed clusters [M3Fe–4S] with potential exogenous ligands contained in the electrolyte. In this paper we report investigations of the equilibria and kinetics of rapid and reversible binding of an exogenous ligand, 1-hydroxyethane-2-thiolate, at oxidized and reduced forms of the transformed [4Fe–4S] cluster in Fd III. (Interestingly, the parent reagent 2-mercaptoethanol is commonly used as a biological reducing agent.) Such activity produces dramatic modulation of the cluster's reduction potential, thus providing a simple demonstration of chemistry that is relevant to the question of redox-linked conformational coupling in proteins.

Experimental Section

Ferredoxin III from *D. africanus*, strain Benghazi (NCIB 8401), was isolated as described previously[37] and stored as frozen pellets in liquid nitrogen. Ferredoxin solutions were prepared for studies by diafiltration against buffer solutions at 4 °C using an Amicon 8MC unit equipped with a microvolume assembly and a YM5 membrane. Final concentrations were determined using an absorption coefficient of 28.6 mM^{-1} cm^{-1} at 408 nm, and samples had a purity index (A_{408}/A_{280}) of 0.72. The ferredoxin solution (100 μM) contained 0.1 M NaCl (Sigma) and 100 μM EGTA (1,2-bis(2-aminoethoxy)ethane-*N,N,N′,N′*-tetraacetic acid; Aldrich) and was buffered with 20 mM Hepes (Sigma) at pH 7.4. Purified water of resistivity ~18 MΩ cm (Barnstead Nanopure) was used in all cases. For voltammetry the buffer–electrolyte solutions consisted of 0.2 M NaCl containing 2 mM neomycin and 20 mM HCl adjusted to the desired pH with Tris (Sigma) at 0 °C. Neomycin sulfate (Sigma) was added as a 0.2 M stock solution adjusted to pH 7. Polymyxin B sulfate (Sigma) (used in preparation of films for certain experiments) was dissolved in water to give a stock solution of 12 mg/mL at pH 7.4. Solutions of 2-mercaptoethanol (1-hydroxyethane-2-thiol; ICN) were prepared immediately prior to experiments using the buffer–electrolyte and the pH was adjusted to the required value at 0 °C by addition of Tris. Aliquots of Fe(II) ($(NH_4)_2Fe(SO_4)_2 \cdot 6H_2O$; Aldrich) were taken as required from concentrated, Ar-purged stock solutions kept in a glovebox.

Electrochemical experiments were carried out with an all-glass cell which consisted of a centrally located reference compartment, linked radially by Luggin capillary arms to four small-volume sample pots.[36] The saturated calomel reference electrode (SCE) was positioned in the central compartment and maintained at 22 °C (at which we have assumed E(SCE) is 243 mV versus the standard hydrogen electrode (SHE)). The auxillary electrode in each sample pot was a piece of Pt gauze positioned opposite to the Luggin tip. The sample pots, holding 500 μL of buffer–electrolyte containing the reagents of interest, were immersed in a cooling bath maintained at 0 °C and the solutions deoxygenated by passing humidified, O_2-purged argon through them.

Pyrolytic graphite 'edge' (PGE) working electrodes consisted of a piece of pyrolytic graphite (Le Carbone, Portslade, Sussex, UK) mounted into a Teflon sheath with the *a–b* plane perpendicular to the solution interface. The electrode (surface area typically 0.18 cm^2) was polished prior to each experiment with aqueous alumina slurry (Buehler micropolish 1.0 μM) and sonicated extensively to remove traces of Al_2O_3. Films were prepared by coating the freshly polished electrode surface with ca. 1 μL of chilled protein solution prepared as described above containing 2 mM neomycin (in certain cases, polymyxin was used in place of neomycin). The coated electrode was then placed promptly into the electrolyte solution of interest. At all times during voltammetry, the PGE surface was positioned close to the Luggin tip. For some experiments, a rotating disk electrode was used, This was constructed in a manner similar to that for the regular electrode, but the sheath was modified to interface with an electrode rotation system (Model 636, Princeton Applied Research).

Cyclic voltammetry was carried out with an Ursar Instruments potentiostat and voltammograms recorded with a Kipp and Zonen XY recorder. Formal reduction potentials $E^{\circ\prime}$ were determined from the average of reduction (cathodic) and oxidation (anodic) peak potentials $(E_{pc} + E_{pa})/2$. All values are given with reference to the standard hydrogen electrode (SHE). Determination of the pK_a for 2-mercaptoethanol under the conditions of the voltammetric experiment was carried out by pH titration of a 50 mM mercaptoethanol solution in 0.2 M NaCl at 0 °C (i.e. similar to conditions of voltammetric experiments) using a NaOH solution previously standardized against oxalic acid.

Digital simulations of voltammetry, as outlined in the Appendix, were based upon the explicit model approach.[38] An iterative program was written in the C language and executed on an SGI 320 computer; this enabled rapid acquisition of simulated results.

Preparations of samples for spectroscopy were carried out in an anaerobic glovebox (O_2 < 1 ppm). EPR spectra were recorded at UEA using a Bruker ER-200D X-band spectrometer equipped with a helium flow cryostat (ESR-9, Oxford Instruments, plc). Low-temperature magnetic circular dichroism (MCD) measurements were made using a JASCO J-500D dichrograph and split-coil superconducting magnet SM-4. Procedures for measuring EPR and MCD spectra have been described previously.[33]

Results and Discussion

Voltammetric Detection of a Specific Reaction of the Transformed [4Fe–4S] Cluster with Exogenous Ligand. Definitions of the redox couples observed for 7Fe and 8Fe forms of Fd III are given in Table I. The following experiments were carried out with the 8Fe form. Films were obtained by coating an electrode with the 7Fe protein as described above and cycling the applied potential between −250 and −850 mV in a buffer–electrolyte solution (pH values 8–8.5) containing 100 or 180 μM Fe(II). Cycling was continued until the [3Fe–4S]-to-[4Fe–4S] cluster transformation was complete (typically 1 min), as evidenced from the disappearance of couple C′.[12] The electrode was then transferred to a second sample pot (this was performed with the

(33) Armstrong, F. A.; George, S. J.; Cammack, R.; Hatchikian, E. C.; Thomson, A. J. *Biochem. J.* **1989**, *264*, 265.
(34) Armstrong, F. A.; Butt, J. N.; George, S. J.; Hatchikian, E. C.; Thomson, A. J. *FEBS Lett.* **1989**, *259*, 15.
(35) Armstrong, F. A. *Struct. Bonding* **1990**, *72*, 137. Armstrong, F. A. In *Advanced Inorganic Chemistry*; Cammack, R., Sykes, A. G., Eds.; Academic Press: 1992; Vol. 38, p 117.
(36) Armstrong, F. A.; Butt, J. N.; Sucheta, A. *Meth. Enzymol.*, in press.
(37) Hatchikian, E. C.; Bruschi, M. *Biochim. Biophys. Acta* **1981**, *634*, 41.
(38) Feldberg, S. W. *Electroanal. Chem.* **1969**, *3*, 199.

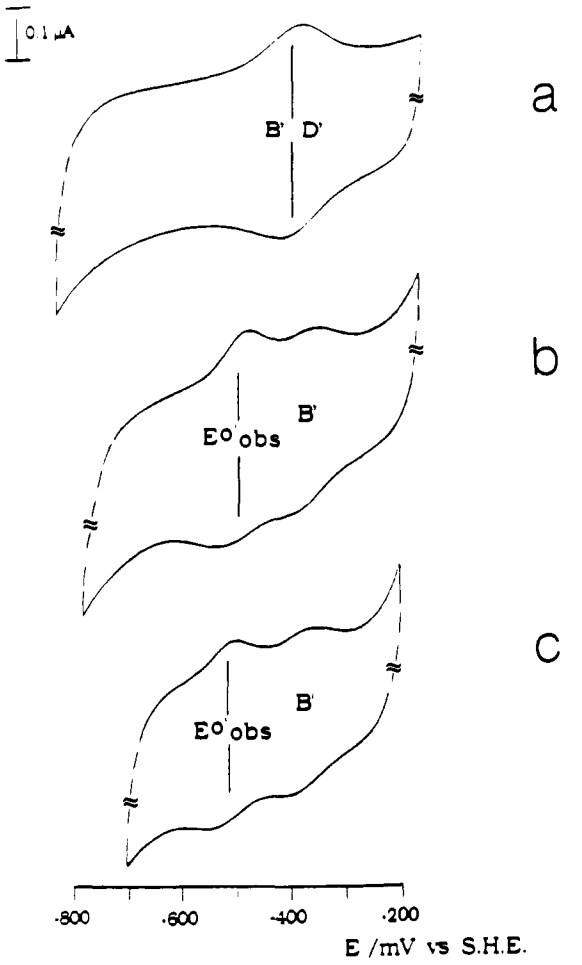

Figure 1. Voltammograms of films of 8Fe Fd III recorded at 0 °C, pH 8.0, with various amounts of mercaptoethanol in the cell. All solutions contained 180 μM Fe(II). Scan rate 10 mV/s. Other conditions as described in text. Mercaptoethanol concentrations (thiolate concentrations given in parentheses): (a) 0 mM; (b) 168 (2.6) mM; (c) 536 (8.4) mM. Couple B' is due to the indigenous (stable) $[4Fe–4S]^{2+/1+}$ cluster. $E^{\circ\prime}_{obs}$ indicates the position of the new couple (see text).

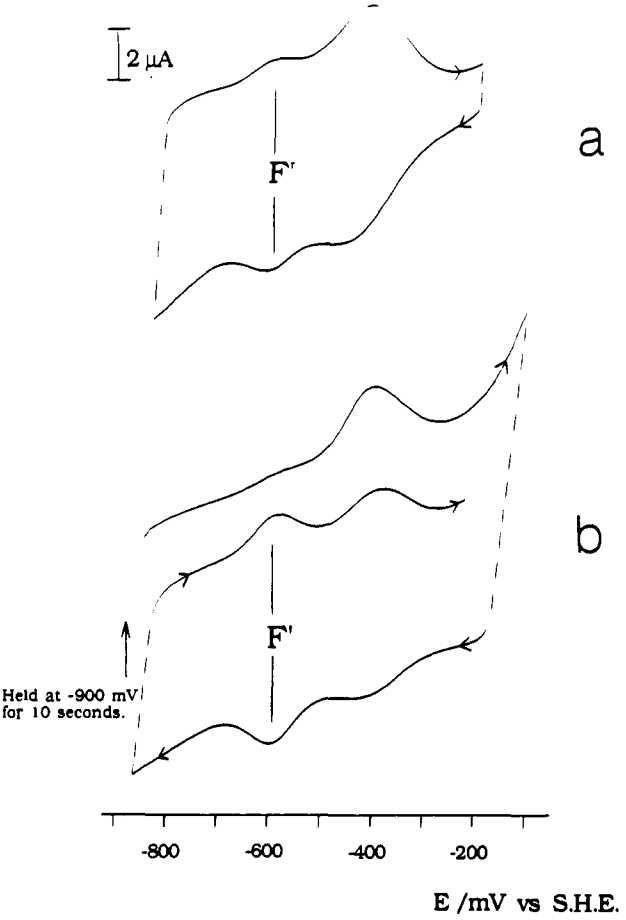

Figure 2. Voltammograms of films of 8Fe Fd III recorded at 930 mV/s in buffer–electrolyte (pH 8.3) containing 100 μM Fe(II). Temperature 0 °C. Other conditions as given in text. (a) Scan after multiple cycling in 1 mM mercaptoethanol (thiolate concentration 31 μM). (b) Scan in 68 mM mercaptoethanol (thiolate concentration 2.1 mM) initiated after holding at -900 mV for 10 s. Subsequent reduction and reoxidation scans are shown. These do not change during further repetitive cycling. The position of couple F', proposed to be due to the ligated transformed cluster L-$[4Fe–4S]^{2+/1+}$, is shown.

electrode remaining connected at a potential of −550 mV) which contained buffer–electrolyte with various concentrations of 2-mercaptoethanol at pH values in the range 8.0–8.5. These solutions also contained 100 or 180 μM Fe(II) to prevent net release of Fe from the transformed $[4Fe–4S]^{2+}$ cluster.[39]

Figure 1 shows voltammograms obtained under conditions of slow scan rate (10 mV/s) for solutions containing increasing concentrations of 2-mercaptoethanol at pH 8.0. It can be seen that the original pair of superimposed waves, corresponding to couple B' (the indigenous $[4Fe–4S]^{2+/1+}$ cluster) and D' (the transformed $[4Fe–4S]^{2+/1+}$ cluster) separates into two pairs. One of these wave pairs remains close to the original position, there being just a small shift to higher potential (from −396 to −385 mV). The other pair (in which the reduction wave is noticeably broader than the oxidation wave, see below) undergoes a marked shift to lower potential ($E^{\circ\prime}_{obs}$) as the mercaptoethanol concentration or pH is increased. By inspection, it was ascertained that the total faradaic charge passed in a single sweep is conserved and that each component of the separated waves has approximately equal area. Provided Fe(II) was present in the electrolyte, there was no reappearance of couples A' and C'. On the other hand, upon further transfer to a sample pot containing buffer–electrolyte without Fe(II) or mercaptoethanol, couples A' and C' reappeared, thereby signalling regeneration of the original 7Fe ferredoxin and demonstrating the reversibility of the sequence of reactions. As determined from voltammograms recorded in the absence of the film of ferredoxin, no waves attributable to redox reactions of the Fe(II)/mercaptoethanol electrolyte were observed in the same potential range. Most importantly, control experiments carried out with an *untransformed* (7Fe) ferredoxin film showed *no change* in the voltammogram upon transfer to the mercaptoethanol solution. The mercaptoethanol-insensitive and mercaptoethanol-sensitive waves of transformed Fd III may thus be assigned to couples B' and D', respectively. These results enable us to conclude that the voltammetric response to mercaptoethanol depends unequivocally upon the presence of the *transformed* [4Fe–4S] cluster. The obvious implication is that this cluster is the specific target of interaction. To check that the sensitivity to mercaptoethanol was not restricted to adsorbed protein molecules, voltammograms were measured under slow scan conditions for a solution of Fd III (0.18 mM) in the presence of Fe(II) (2 mM), before and after addition of mercaptoethanol (to 72 mM). The simple, almost classical voltammogram[8] obtained in the absence of thiol (i.e. a reversible, diffusion-controlled response that is actually composed of two one-electron couples B and D having very similar reduction potentials) became severely distorted through flattening of the peaks and marked broadening in the direction of negative potential.

Figure 2 shows voltammograms obtained under conditions of rapid scan rate, i.e. 930 mV/s, for solutions containing two dif-

(39) Complex formation between Fe(II) and 1-hydroxyethane-2-thiolate (2-mercaptoethanol) is weak and does not promote Fe release from the protein or substantially alter the available ligand concentration. We found no evidence for interference with the voltammetry experiments. See: Armanet, J. P.; Merlin, J. C. *Bull. Soc. Chim. Fr.* **1961**, 440.

Scheme II

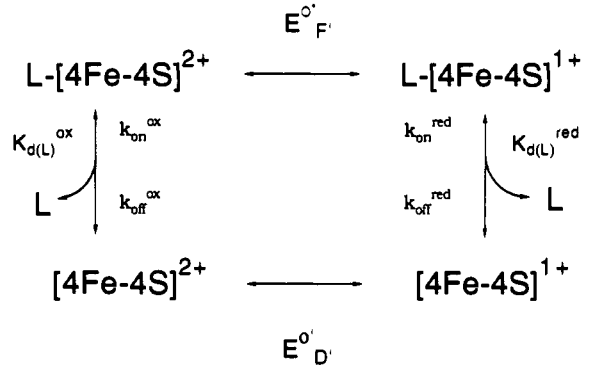

ferent concentrations of mercaptoethanol at pH 8.3. (In order to observe the effects of varying concentration, levels are lower than those used in the slow-scan experiments.) As before, two redox couples are observed. However the major effect of varying the thiol concentration is now to change the relative amplitudes of each wave rather than the potential position. We refer to the 'new' low-potential couple as F'. As the mercaptoethanol concentration is increased, the size of the oxidation wave of F' approaches that of its corresponding reduction wave, while the reduction potential appears constant at −585 ± 15 mV. The faradaic charge passed per sweep is conserved through complementary variations in the size of the signals due to the couple with $E^{\circ\prime} \sim$ −396 mV. Voltammograms recorded after several cycles were identical to the initial scan commenced from the high-potential limit. On the other hand, as shown in Figure 2b, the initial oxidative sweep as commenced from the low-potential limit or after a 10-s hold at ca. −900 mV showed only a trace amount of oxidation wave F', with the remainder of the oxidation current appearing in the proximity of wave B'.

Determination of Equilibrium (Dissociation) Constants for Thiolate Binding to Oxidized and Reduced Forms of the Transformed [4Fe–4S] Cluster. These results can be explained on the basis of a reversible ligand-binding reaction that is coupled to electron transfer as shown in Scheme II. The dissociation constants for oxidized and reduced [4Fe–4S] clusters are defined as in eqs 1 and 2

$$K_{d(L)^{ox}} = \{[4Fe\text{–}4S]^{2+}\}\{L\}/\{L\text{-}[4Fe\text{–}4S]^{2+}\} \quad (1)$$

$$K_{d(L)^{red}} = \{[4Fe\text{–}4S]^{1+}\}\{L\}/\{L\text{-}[4Fe\text{–}4S]^{1+}\} \quad (2)$$

where $\{[4Fe\text{–}4S]^{2+}\}$ etc. are surface populations of a particular species and {L} is the concentration of ligand in the solution. With a slow scan rate, changes in ligation occur rapidly compared to the experimental time frame and conditions approaching equilibrium are maintained. (This is analogous to the situation that holds for potentiometric measurements.) The apparent reduction potential $E^{\circ\prime}_{obs}$ is dependent upon ligand concentration according to eqs 3 and 4

$$E^{\circ\prime}_{obs} = E^{\circ\prime}_{D'} + (2.303RT/F) \log \{(1 + [L]/K_{d(L)^{red}})/(1 + [L]/K_{d(L)^{ox}})\} \quad (3)$$

$$E^{\circ\prime}_{F'} = E^{\circ\prime}_{D'} + (2.303RT/F) \log (K_{d(L)^{ox}}/K_{d(L)^{red}}) \quad (4)$$

where $E^{\circ\prime}_{D'}$ is the reduction potential of the native transformed cluster and $E^{\circ\prime}_{F'}$ is the reduction potential of the exo-ligated cluster (couple F'). A plot of $E^{\circ\prime}_{obs}$ against log [L] is thus predicted to be sigmoidal with asymptotic limits at $E^{\circ\prime}_{D'}$ for $[L] \ll K_{d(L)^{ox}}$ and at $E^{\circ\prime}_{F'}$ for $[L] \gg K_{d(L)^{red}}$.

The effect of pH was incorporated through equation 5. The applicability of this equation over a range of 2-mercaptoethanol concentrations and pH values showed that the thiolate anion, not the thiol, is the active ligand. We used the value $K_H = 10^{-9.8}$,

$$[\text{thiolate}] = [\text{thiol}]_{total}/(1 + [H^+]/K_H) \quad (5)$$

determined as described in the Experimental Section. The resulting plot of $E^{\circ\prime}_{obs}$ against log [thiolate] is shown in Figure 3. It was not possible to measure $E^{\circ\prime}_{obs}$ over a wide range of thiolate concentrations. At low levels a clear separation from couple B' was not observed. At thiolate concentrations sufficiently high for $E^{\circ\prime}_{obs}$ to approach the limit of $E^{\circ\prime}_{F'}$, all voltammetric signals vanished during the course of a slow scan, indicating desorption of protein or degradation of clusters. However, since $E^{\circ\prime}_{F'}$ could be determined easily from the rapid scan experiments (−585 ± 15 mV) and $E^{\circ\prime}_{D'}$ is known to reasonable accuracy (−396 ± 15 mV), the computation of $K_{d(L)^{ox}}$ and $K_{d(L)^{red}}$ from nonlinear regression analysis was straightforward. A good fit was obtained over a range of pH values, giving $K_{d(L)^{ox}} = 28 \pm 9$ μM and $K_{d(L)^{red}} = 97 \pm 17$ mM.

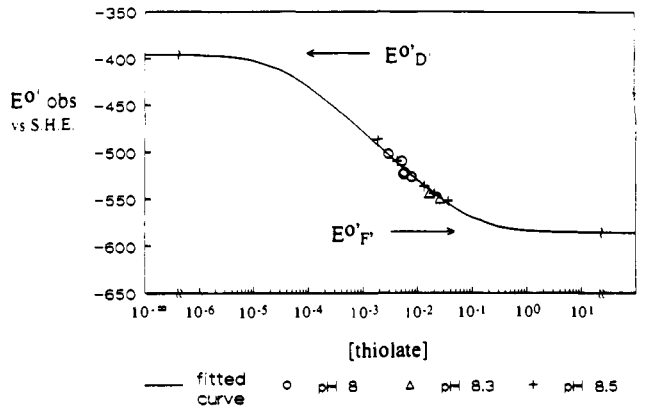

Figure 3. Plot of $E^{\circ\prime}_{obs}$ as a function of log [thiolate] measured at various pH values. Conditions as described in text and as given for Figure 1. Average values of $E^{\circ\prime}_{obs}$ were obtained from voltammograms recorded at 2, 5, and 10 mV/s. Thiolate concentrations were determined from eq 5. The fitted curve is the result of nonlinear regression analysis based upon eq 3 with $E^{\circ\prime}_{F'}$ (measured directly and defined by eq 4) = −585 mV.

Kinetics of Reversible Ligand Binding. Figure 4 shows voltammetry at an intermediate scan rate (191 mV/s) obtained under conditions of increasing mercaptoethanol concentration at pH 8.3. These each show a *third* oxidation wave (indicated by ✱) which shifts to lower potential as the mercaptoethanol concentration is raised. Upon holding the potential for 10 s at the lower limit of the range, the reoxidation wave of couple F' disappears almost completely while the amplitude of the new feature is proportionately increased. The position of the third wave shifts to more negative potential as the scan rate is lowered, but does not vary with pH over the range used, provided the mercaptoethanol concentration is adjusted to give the same final concentration of thiolate as described by eq 5. Figure 5 shows the magnitude of the potential shift ΔE (i.e. the position of the third peak relative to the reduction potential $E^{\circ\prime}_{D'}$ of the untransformed $[4Fe\text{–}4S]^{2+/1+}$ cluster) as a function of scan rate and thiolate concentration. In a set of control experiments, polymyxin[40] was used as the coadsorbate instead of neomycin, and the electrode was rotated at rates up to 3000 rpm.[41] Values of ΔE observed in these experiments were identical (±5 mV) to those obtained with neomycin.[42]

This unusual voltammetry reveals important kinetic information. Consequently a model was devised, incorporating the four rate constants for exogenous ligand binding and release at oxidized and reduced forms of the cluster. The model was executed as a simulation program, as outlined in the Appendix to this article.

(40) Hayashi, K.; Suzuki, T. *Bull. Inst. Chem. Res., Kyoto Univ.* **1965**, *43*, 259.

(41) We found that neomycin-coated ferredoxin films desorb rapidly if the electrode is rotated. To stabilize the protein film at the rotating disk electrode, we used polymyxin (in place of neomycin) at a concentration of 48 μg/mL (approximately 30 μM) in the protein solution used for film formation.

(42) Polymyxin-coadsorbed films of 8Fe Fd III in the absence or presence of thiol displayed voltammetric peaks that were each shifted ca. 15 mV to more positive potentials as compared to those of films formed with neomycin. This probably reflects differences in the potential profile across the electrode–film interface; significantly, the kinetics of ligand binding are unaffected.

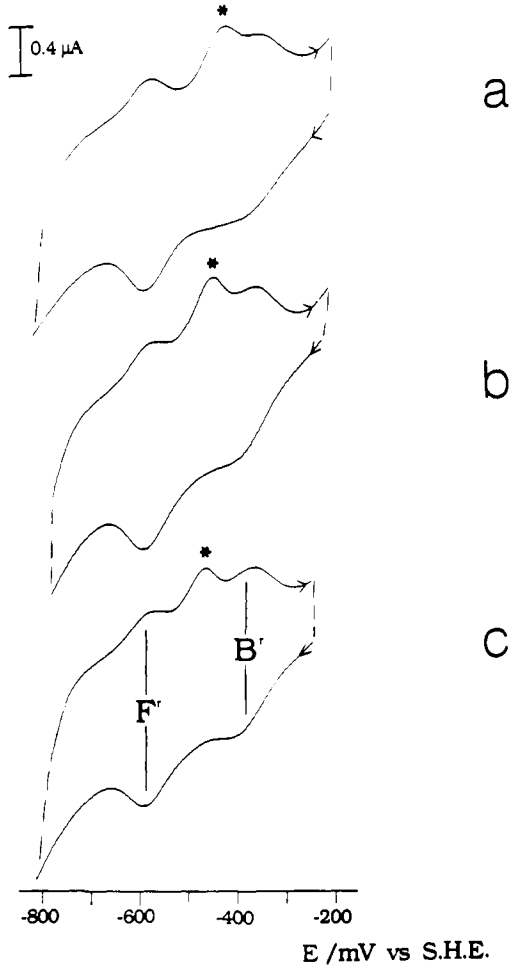

Figure 4. Voltammograms of 8Fe Fd III recorded at 191 mV/s with various levels of mercaptoethanol, showing the appearance of the third oxidation wave ✱. Conditions are as for Figure 2. Concentrations of mercaptoethanol (that of thiolate given in parentheses) in mM: (a) 68 (2.1); (b) 238 (7.3); (c) 443 (13.6). Couple F′ is the ligated, transformed cluster L-[4Fe–4S]$^{2+/1+}$.

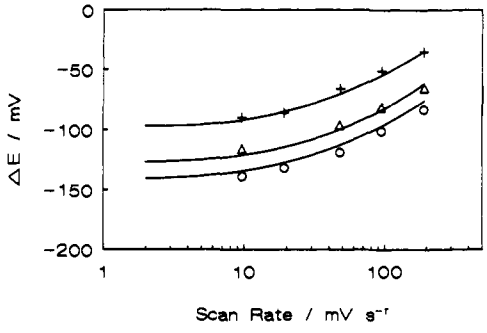

Figure 5. Dependence of ΔE (the separation between the peak position determined for oxidation wave ✱ and the reduction potential of the parent couple D′ ($E^{\circ\prime}_{D'}$)) upon scan rate, at three different concentrations of the ligand 1-hydroxyethane-2-thiolate: +, 2.1 mM; Δ, 7.3 mM; O, 13.6 mM. Solid lines connect points generated by computer simulation at the same concentrations.

The underlying assumptions were (i) a homogeneous monolayer of non-interacting protein molecules, each containing one stable [4Fe–4S] cluster and one reactive (transformed) [4Fe–4S] cluster in either a ligand-free or ligated state in accordance with Scheme II; (ii) exchange of ligand L between the transformed clusters and the adjacent solution with the ligand concentration buffered (and thus effectively invariant with distance from the electrode) by rapid equilibration with the concentrated thiol pool; and (iii) all electrochemical and chemical reactions occurring within the boundaries of this layer. Several values of the electrochemical rate

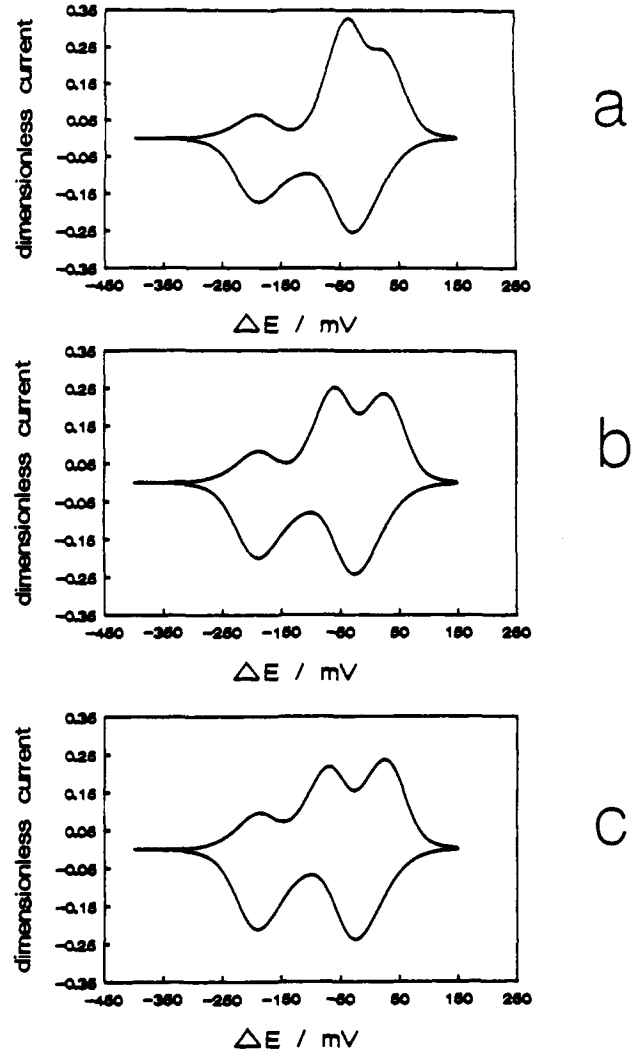

Figure 6. Computer simulations of voltammograms at a scan rate of 191 mV/s with the following rate constants: $k_{off^{red}} = 0.3\ s^{-1}$, $k_{off^{ox}} = 0.9\ s^{-1}$, $k_{on^{red}} = 3.09\ M^{-1}\ s^{-1}$, and $k_{on^{ox}} = 3.2 \times 10^4\ M^{-1}\ s^{-1}$. Most satisfactory electrochemical rate constants for couples B′, D′, and F′ are 5, 50, and 20 s^{-1}. Concentrations of thiolate (mM): (a) 2.1; (b) 7.3; (c) 13.6.

constants were tested. These were first-order rate constants, using the formalism of Laviron.[43]

The chief criterion that we used to match experiment and simulation was the potential shift ΔE. The rate constants providing the best fit over a range of thiolate concentration were $k_{off^{red}} = 0.3\ s^{-1}$, $k_{off^{ox}} = 0.9\ s^{-1}$, $k_{on^{red}} = 3.09\ M^{-1}\ s^{-1}$, and $k_{on^{ox}} = 3.2 \times 10^4\ M^{-1}\ s^{-1}$, and electrochemical rate constants[44] of 5, 50, and 20 s^{-1}, respectively, for couples B′, D′, and F′. In straightforward terms, the third oxidation peak arises because, for this time frame, the electrochemically facile oxidation of non-thiolate-ligated clusters couples effectively with the ensuing rapid, spontaneous binding of thiolate; in electrochemical terminology this is an 'EC' reaction.[45] The solid lines shown in Figure 5 indicate values of ΔE

(43) Laviron, E. *J. Electroanal. Chem. Interfacial Electrochem.* **1979**, *101*, 19.

(44) The electrochemical rate constants for couples B′ and F′ were estimated from experimental voltammograms by inspection of the respective separations of peaks for oxidation and reduction under high-thiolate conditions at a scan rate of 1 V/s. The electrochemical rate constant adopted for couple D′ was the value best conforming to the final simulation. The errors involved are not clear and, to a great degree, changes in the electrochemical rate constants did not alter the general appearance of the simulated voltammograms. However, they did contribute to minor details. For example, the use of a much larger rate constant for couple F′ caused oxidation and reduction peaks to have a negative potential separation; experimentally, this was never observed.

(45) Bard, A. J.; Faulkner, L. R. In *Electrochemical Methods; Fundamentals and Applications*; Wiley: New York, 1980; p 429.

Table II. Compilation of Equilibrium (Dissociation) Constants ($K_{d(L)}$) and Rate Constants for Binding of 1-Hydroxyethane-2-thiolate at the Transformed [4Fe–4S] Cluster of Ferredoxin III (*D. africanus*)[a]

cluster	$K_{d(L)}$ (M)	k_{on} (M^{-1} s^{-1})	k_{off} (s^{-1})
oxidized $[4Fe–4S]^{2+}$	28 (9) × 10^{-6}	3.2 (1.1) × 10^{4}	0.9 (0.3)
reduced $[4Fe–4S]^{1+}$	0.097 (0.017)	3.09 (1.03)	0.3 (0.1)

[a] Temperature 0 °C, pH 8.0–8.5 (Tris), 0.2 M NaCl. Estimated errors are given in parentheses. Errors in equilibrium constants were estimated from consideration of the uncertainties in thiolate concentration and the values of $E^{\circ\prime}_{D'}$ and $E^{\circ\prime}_{F'}$ and of the standard deviation in the nonlinear regression fit to eq 3. Errors in rate constants were correlated; i.e., a simulation showing an erroneous value of $k_{off^{ox}}$ would show disagreement between the observed and simulated parameters of voltammetry (peak positions and relative peak amplitudes) only if $k_{off^{red}}$ remained correct. Simulation with both $k_{off^{ox}}$ and $k_{off^{red}}$ in error could yield voltammograms approximating the experiment better than in the case of only one constant being in error. The rate constants presented here were arrived through a systemmatic search covering $k_{off^{red}}$ in the range 0.02–1.0 s^{-1} (estimated from inspection of experimental results) with the experimental equilibrium constants $K_{d(L)^{ox}}$ and $K_{d(L)^{red}}$ serving as guidelines.

obtained by simulation using the above rate constants. The agreement is good; experimental results at each scan rate were close to simulated values over the entire range of thiolate concentration used,[46] at pH values between 8.0 and 8.5, thus showing that the kinetics are first-order with respect to thiolate and are otherwise independent of pH. The simulated and observed results remained in agreement for examples in which the scan range was extended to more negative potentials and for scans commenced from the low-potential limit. The position of the third oxidation wave was found to be independent of these experimental variables. Equilibrium and kinetic data for ligand binding are compiled in Table II.

Simulations corresponding to the experimental thiolate concentrations used in Figure 4 are shown in Figure 6. An obvious discrepancy is that the component waves of couple B′ appear much broader in the experiment than in the simulations. While it was difficult to make allowances for the variable sloping background in our experimental results, this observation can readily be accounted for. We have previously suggested[12] that such broadening reflects inhomogeneity or (less likely) interaction among the indigenous [4Fe–4S] clusters in the film. The experimentally observed half-height width for the waves of couple B′ is typically 120 mV or more. However, the simulations conform to the theoretical value[43] of 83 mV that is appropriate for 0 °C. We noted also that the broadened reduction and sharpened oxidation waves that are observed experimentally for the couple $E^{\circ\prime}_{obs}$ at 10 mV/s (Figure 1b,c) emerged naturally in the appropriate simulation. Although equilibrium thus appears not to be fully established even at this slow scan rate, the error in determining the value of $E^{\circ\prime}_{obs}$ was considered to be insignificant.

Calculated Stability Limits of Cluster Species in Scheme II and Effects of Mercaptoethanol on the EPR and MCD Spectra of Reduced Protein. Our proposal that the transformed cluster undergoes rapid and reversible coordination of ligands has thus far rested entirely upon electrochemical evidence, that is, our observations of reproducible, systemmatic changes in the appearance of the voltammetric signals originating from couple D′ and our ability to account quantitatively for all the experimental data using the model of Scheme II. From these data we could now determine the limits of stability of each of the four species involved, i.e. $[4Fe–4S]^{2+}$, $[4Fe–4S]^{1+}$, L-$[4Fe–4S]^{2+}$, and L-$[4Fe–4S]^{1+}$, as a function of thiolate concentration and applied potential. Computed distributions of cluster species over a wide range of ligand concentrations at three potential values are shown in Figure 7. For a potential of −350 mV and more positive values, it is clear that the oxidized thiolate-bound cluster is the predominant species at thiolate concentrations above $K_{d(L)^{ox}}$, i.e. ~10^{-4} M. By contrast, at −650 mV the other limiting situation is approached; the reduced thiolate-bound cluster becomes the predominant species only once the thiolate concentration is in excess of $K_{d(L)^{red}}$, i.e. ~0.1 M. It is seen further that a thiolate concentration well in excess of 1 M is required to achieve near-saturative binding to the reduced cluster, while a concentration as low as 10^{-3} M produces a negligible degree of binding. The middle chart shows the situation which would prevail at −550 mV, i.e. at the practical limit for reduction of a redox center by dithionite. We observe that it is not possible to obtain more than 20% of the cluster population in the thiolate-bound reduced form at any thiolate concentration. With these limitations in mind we undertook studies to examine the effect of mercaptoethanol upon the EPR and MCD spectra of the reduced 8Fe protein. Three experiments were carried out.

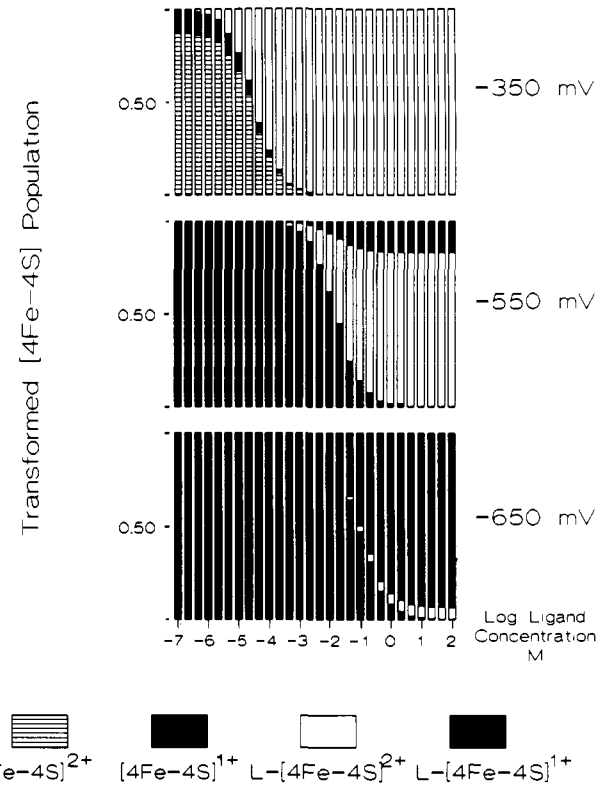

Figure 7. Distributions of species $[4Fe–4S]^{2+}$, $[4Fe–4S]^{1+}$, L-$[4Fe–4S]^{2+}$, and L-$[4Fe–4S]^{1+}$ as participating in Scheme II. For each case, fractions of the total cluster population are computed on the basis of the dissociation constants and reduction potentials as determined in this study. They are displayed as a function of the concentration of 1-hydroxyethane-2-thiolate at three different values of applied potential.

In the first study, a sample of 8Fe ferredoxin (1.1 mM in 0.1 M NaCl, 20 mM Tris, pH 8.6) was prepared as described previously[8] and reduced with a large excess of sodium dithionite (100 mM). The EPR spectrum of this sample showed the expected rhombic signals centered at g = 1.93 (from the indigenous $[4Fe–4S]^{1+}$ cluster with $S = {}^1/_2$) and the signal at g = 5.27 (from the transformed $[4Fe–4S]^{1+}$ cluster with $S = {}^3/_2$). Upon addition of mercaptoethanol to a total concentration of 3.55 M (giving a thiolate concentration of 0.21 M), the sample turned from golden brown to black and a black precipitate came down. The EPR spectrum revealed loss of both signals and the appearance of a signal at g = ~10. The latter signal could be observed also in similar solutions of Fe(II), mercaptoethanol, and dithionite and is presumably due to high-spin Fe(II) (S = 2) in a tetrahedral thiolate site. It could be concluded that mercaptoethanol at this

(46) At highest thiolate concentration, the experimental values of ΔE appear marginally higher than those from the simulation. The discrepancy, in the order of 5 mV, is however within experimental error, and the effect on rate constants is small. A general idea of the margin of error in determining rate constants is given by our finding that simulations with a two-fold decrease or increase in ligand binding rate constants gave no consistent agreement with the observed voltammetry. A major conclusion of this work, that k_{on} for oxidized and reduced clusters differ by *four orders of magnitude*, is thus unavoidable, even if data are subject to the maximum expected uncertainty.

high concentration causes degradation of both clusters.

In the second study, a sample of 8Fe ferredoxin (1.6 mM in 0.5 M Tris, pH 8.65) was reduced with excess dithionite. The reduced solution showed the expected EPR signals at $g = 1.93$ and 5.27. Then mercaptoethanol was added to give a final concentration of 0.72 M, corresponding to 42 mM thiolate. Some precipitate was observed. The EPR spectrum showed that the signal at $g = 5.27$ was lost completely while the signal at $g = 1.93$ remained at equal integrated intensity with some changes in line shape.

In the third study, a sample of 8Fe ferredoxin (0.55 mM in 0.1 M NaCl, 20 mM Tris, pH 8.6) was reduced with a small excess of dithionite (1.4 mM). The EPR spectrum showed the expected signals at $g = 1.93$ and 5.27. Then mercaptoethanol was added to give a final concentration of 0.10 M, corresponding to 6.6 mM thiolate. No precipitate was observed. The EPR spectrum showed that the integrated intensity of the signal at $g = 1.93$ was unchanged after correction for dilution. Using this signal as a standard, it was determined that the relative intensity of the signal at $g = 5.27$ had decreased to 0.35 of its original value. No new signals were observed although there was some change in line shape at $g = 1.93$. The sample was then thawed, ethanediol was added to 50% v/v, and portions were used for EPR and MCD spectroscopy. The EPR spectrum showed that the signal at $g = 5.27$ was restored to 0.65 of its original value relative to the signal at $g = 1.93$. The MCD spectrum was identical to that of the reduced 8Fe protein but with an intensity equivalent to only 55–65% of that expected if all clusters remained reduced. There was no evidence for formation of $[3Fe–4S]^0$, i.e. from release of Fe.

These observations can be explained on the basis of the distribution diagrams given in Figure 7. In the first case, our inability to prepare a sample of the Kramers system L-$[4Fe–4S]^{1+}$ stems from the weakness of interaction of $[4Fe–4S]^{1+}$ with thiolate. This necessitates a very high concentration of the thiolate in solution, in addition to a large excess of dithionite for achieving adequate reducing power. Not surprisingly, we found that such conditions instead induce rapid loss of the cluster. The second experiment also illustrates this problem, although it appears that the indigenous cluster survives the less harsh treatment. The third experiment is more subtle but now provides indirect evidence for thiolate binding. The partial decrease in intensity of the signal at $g = 5.27$ is explained by spontaneous reoxidation of the transformed $[4Fe–4S]^{1+}$ cluster. This process is favored by the stabilization afforded to the oxidized cluster by the binding of thiolate. The required oxidation equivalents originate most likely from the SO_2/SO_3^{2-} products of dithionite oxidation. The increase in relative intensity at $g = 5.27$ which is then observed upon addition of ethanediol shows that the reaction is reversible under these conditions of relatively low thiol concentration. Such an increase is indeed expected, since ethanediol addition dilutes the sample, lowering the thiolate concentration by 50%. The MCD spectra, again indirectly, support this proposal.

General Comments. The most reasonable interpretation of the results is that thiolate binding occurs specifically at the labile Fe subsite. The alternative possibility, that the transformation from a [3Fe–4S] to [4Fe–4S] cluster activates another Fe subsite toward ligand exchange, must be regarded as unlikely. At present we are uncertain of the identity of the ligand X that is normally coordinated to the reactive Fe subsite (see Scheme I). The strongest candidates are the carboxylate from Asp-14 (which occupies a position that would normally be a cysteine in typical [4Fe–4S] clusters) or a water molecule (H_2O or OH^-). We have noted[47] that values of the $[4Fe–4S]^{2+/1+}$ reduction potential ($E^{o\prime}_D$) are essentially independent of pH over the range 5–8. Furthermore, we have recently determined[48] that formation of $[M3Fe–4S]^{2+}$ species from $[3Fe–4S]^0$ and M (Fe or Zn) is dependent upon deprotonation of a group having $pK = 4.9$. These results suggest involvement of a carboxylate, either directly as a ligand or by assisting the coordination of a water molecule through hydrogen bonding or by stabilizing a particular protein conformation. Of alternatives to cysteine as natural ligands to [4Fe–4S] clusters in proteins, only water (or hydroxide) has precedent. The catalytic Fe subsite of the $[4Fe–4S]^{1+}$ cluster in pig-heart mitochondrial aconitase is coordinated to a OH^- that becomes protonated upon binding substrate.[5,6] Water (or hydroxide) is also proposed to be the non-cysteine ligand in the [4Fe–4S] cluster formed in the ferredoxin from *P. furiosus*.[30]

The kinetic origin of the much stronger interaction of 1-hydroxyethane-2-thiolate with the oxidized cluster $[4Fe–4S]^{2+}$ (and the ca. 200-mV decrease in reduction potential) can now be identified as a large enhancement in the *on* rate. Binding of thiolate to the oxidized cluster indeed occurs some ***4 orders of magnitude*** more rapidly than does binding to the reduced cluster. By contrast, rates of dissociation of thiolate from $[4Fe–4S]^{2+}$ and $[4Fe–4S]^{1+}$ are similar to within a factor of ≤ 5. The kinetics do not depend upon the identity of the coadsorbate: neomycin, an aminocyclitol, gives the same results as polymyxin,[40] which is a cyclic oligomer of amino acids and 1,4-diaminobutyric acid. Films formed with polymyxin are much more stable, as determined by the very slow rate of signal loss, suggesting a marked decrease in the mobility of the adsorbed protein. Furthermore, the fact that results are unaffected by electrode rotation at high frequency shows that the kinetics are not limited by mass transport effects. Thus we are certain that the kinetics reflect an intrinsic property of the protein's active site and are not dependent upon intermolecular interactions within the film. A strong donor ligand is expected to form a stronger bond with the more electron-poor *oxidized* cluster. Consequently, the observation that ligand-exchange activity is much enhanced for the *oxidized* cluster implies that cluster–ligand bond *rupture* cannot be rate limiting for any of the reactions. While it is possible that ligand-exchange rates are controlled by the protein, perhaps via a redox-linked conformation change, the most straightforward interpretation is that ligand exchange is associative; i.e. that the rate-determining step is bond formation between the reactive Fe subsite and the incoming ligand. Ligand-exchange reactions of simple tetrahedral Fe(II) and Fe(III) complexes appear to proceed by an associative pathway,[49] and in the absence of steric hindrance, such a mechanism seems most likely for ligand exchange at the cluster.[50] Support for a lack of hindrance from protein residues stems from a recent communication[13] in which we reported that Tl^+ ions exhibit surprisingly rapid and reversible interaction with the parent [3Fe–4S] cluster.

An alternative proposal is that the Fe–X bond is not ruptured and that thiolate binding is additive, resulting in an increase in coordination number, presumably from 4 to 5. This has precedent in the form of the various subsite-differentiated analogues prepared by Holm and co-workers[28,29] and in the observation that the catalytic subsite of the [4Fe–4S] cluster of aconitase increases its coordination number from 4 to 6 upon binding substrate.[6] The ca. 200-mV negative shift in reduction potential upon thiolate binding is indeed consistent with the increase in core electron density that would be expected.[28] The ability to accommodate such a change (in this protein and perhaps more generally) would be required to depend upon the cluster oxidation level.

Reviewing our observations in the light of Scheme II, we are provided with a remarkably simple demonstration of an important feature of biological redox systems, that is, the time-separated coupling of electron transfer to conformational change.[51,52] The

(47) Butt, J. N.; Armstrong, F. A. Unpublished results.

(48) Butt, J. N.; Fuchs, C.; Weck, M.; Armstrong, F. A. Unpublished results.

(49) Pignolet, L. H.; Forster, D.; DeW Horrocks, W., Jr. *Inorg. Chem.* **1968**, *7*, 828. Algra, G. P.; Balt, S. *Inorg. Chem.* **1981**, *20*, 1102. Algra, G.; Balt, S. *Inorg. Chim. Acta* **1983**, *75*, 179.

(50) Very recent studies of the reactions between small molecules such as arenethiolates and an alkanethiolate on the oxidized cluster analogue $[Fe_4S_4(SEt)_4]^{2-}$ in acetonitrile give evidence for both dissociative and associative pathways via three- or five-coordinate intermediates. On-rates are rapid, with $k \geq 1 \times 10^6\ M^{-1}\ s^{-1}$ (personal communication; R. A. Henderson and K. E. Olgieve).

(51) See comments on gated electron transfer in: Fraústo da Silva, J. J. R.; Williams, R. J. P. *The Biological Chemistry of the Elements*; Oxford University Press: 1991.

voltammetric approach provides a powerful tool for resolving these reactions. Viewed merely in the context of an equilibrium, the observed reduction potential varies with ligand concentration (and thus pH). More interestingly, when viewed in terms of a dynamic, nonequilibrium situation, the ca. −200-mV difference between $E^{\circ\prime}_{(D)}$ and $E^{\circ\prime}_{(F)}$ represents the increase (ca. 19 kJ/mol) in free energy that is required to effect reduction of the $[4Fe\text{–}4S]^{2+}$ cluster when thiolate is bound. However, this additional energy is recovered through the spontaneous change in ligation (equivalent to a conformational change) that occurs after reduction. Energized electrochemically, as in a cyclic voltammetry experiment, the thermodynamic cycle described by Scheme II proceeds clockwise. On the other hand, if the system could be energized instead in such a way as to *reverse* the net direction of ligand interchange (i.e. to enforce thiolate binding at the $[4Fe\text{–}4S]^{1+}$ cluster), then such a system would constitute an 'electron pump', as proposed by Job and Bruice.[25] This provides a means by which mechanical energy (an externally induced conformational change) is transduced into electrical energy (increased reducing power). In such a mode, the cycle of Scheme II proceeds *counter*clockwise.

A final note concerns the complementary nature of the picture that is afforded by voltammetry. Our experiments detected a thiolate-ligated form of $[4Fe\text{–}4S]^{1+}$ that could not be generated in bulk solution because its existence at equilibrium requires a very low potential and an extremely high concentration of thiol—conditions that instead induced rapid cluster degradation. Significantly, EPR, the primary tool for investigating Fe–S proteins, depends upon generation of this paramagnetic oxidation level. The oxidized cluster $[4Fe\text{–}4S]^{2+}$ has a diamagnetic ground state, and (from the MCD experiments) it appears that the thiolate-ligated form is also diamagnetic.[53] Spectroscopic methods such as Mössbauer or resonance Raman which are useful in studies of diamagnetic systems are not routinely used for initial studies. It is thus important to be aware that reactivities which are effectively restricted to the oxidized form (in this case having a very much higher affinity for thiolate) could escape attention.

Acknowledgment. This work was supported by grants from the donors of the Petroleum Research Fund, administered by the American Chemical Society (F.A.A.); The National Science Foundation, MCB-9118772 (F.A.A.); and The UK Science and Engineering Research Council (A.J.T.) and by a NATO collaborative research grant, CRG9003 (F.A.A., A.J.T.).

Appendix

The iterative simulation algorithm was based on a model assuming that electrochemical and chemical reactions were confined to a thin, uniform layer adjacent to the electrode. The concentration of the ligand L (C_L) inside this reaction layer was held constant, on the basis of the large buffering capacity of the thiolate/thiol system that was observed experimentally. This property of the solution gave very rapid compensation for changes in C_L due to chemical reactions.

The initial set of concentrations used in the simulation (surface concentrations for the transformed cluster; O = $[4Fe\text{–}4S]^{2+}$, R = $[4Fe\text{–}4S]^{+}$, OL = L-$[4Fe\text{–}4S]^{2+}$, RL = L-$[4Fe\text{–}4S]^{+}$: for the indigenous stable cluster; O′ = $[4Fe\text{–}4S]^{2+}$, R′ = $[4Fe\text{–}4S]^{+}$: and the bulk concentration of L = $HOCH_2CH_2S^-$) were determined from the pertinent equilibrium requirements at the initial potential E_{init}:

$$C_{O'}/C_{R'} = \exp[f(E_{init} - E^{\circ\prime}_{B'})]$$

$$C_O/C_R = \exp[f(E_{init} - E^{\circ\prime}_{D'})]$$

$$C_O C_L/C_{OL} = K_{d(L)^{ox}}$$

$$C_R C_L/C_{RL} = K_{d(L)^{red}}$$

$$C_O + C_R + C_{OL} + C_{RL} = C_{O'} + C_{R'}$$

$$\text{and } C_{tot} = C_O + C_R + C_{OL} + C_{RL} = \text{constant}$$

where $f = nF/RT$. Subsequent iterations followed with a time step Δt set in such a way that concentrations of O′, R′, O, R, OL, and RL did not vary by more than 1% within each iteration. On the basis of the scan rate ν (which was entered as one of the simulation parameters), a new electrode potential was then determined $E^{(1)} = E_{init} + \nu\Delta t$ and components of the dimensionless current ($IRT/n^2F^2A\nu C_{tot}$) arising for couples B′, D′, and F′ were calculated from their respective Butler–Volmer characteristics.

$$I_{B'} = nFAk^\circ_{B'}\{C_{O'}\exp[-\alpha_{B'}f(E^{(1)} - E^{\circ\prime}_{B'})] - C_{R'}\exp[(1-\alpha_{B'})f(E^{(1)} - E^{\circ\prime}_{B'})]\}$$

$$I_{D'} = nFAk^\circ_{D'}\{C_O\exp[-\alpha_{D'}f(E^{(1)} - E^{\circ\prime}_{D'})] - C_R\exp[(1-\alpha_{D'})f(E^{(1)} - E^{\circ\prime}_{D'})]\}$$

$$I_{F'} = nFAk^\circ_{F'}\{C_{OL}\exp[-\alpha_{F'}f(E^{(1)} - E^{\circ\prime}_{F'})] - C_{RL}\exp[(1-\alpha_{F'})f(E^{(1)} - E^{\circ\prime}_{F'})]\}$$

Here, the terms $\alpha_{B'}$, $\alpha_{D'}$, and $\alpha_{F'}$ are electrochemical transfer coefficients considered here to equal 0.5, while $k^\circ_{B'}$, $k^\circ_{D'}$, and $k^\circ_{F'}$ are the characteristic electrochemical rate constants with units of s^{-1} (cf. ref 43). The resultant rates of electrochemical change (I/nFA) were subsequently used to calculate a new set of concentrations for participating species. Next, the chemical reactions were considered; rates of chemical change were calculated from concentrations arising after the electrochemical step:

$$\Delta C_O/\Delta t = k_{off^{ox}}C_{OL} - k_{on^{ox}}C_O C_L$$

$$\Delta C_{OL}/\Delta t = -\Delta C_O/\Delta t$$

$$\Delta C_R/\Delta t = k_{off^{red}}C_{RL} - k_{on^{red}}C_R C_L$$

$$\Delta C_{RL}/\Delta t = -\Delta C_R/\Delta t$$

These variations were used to determine new values of concentrations after the first iteration. The simulation program now proceeded to calculate a new value of potential and repeat all the described steps until the whole potential range of interest was covered. Usually, two segments (descending and ascending) of the potential wave form were simulated. The values of dimensionless current components were sampled for analysis in 2-mV intervals.

(52) Another example of a coupled protein electron-transfer reaction is the reversible pH-linked interconversion between conformers of mitochondrial cytochrome *c*, A voltammetric study of this system has recently been published. Barker, P. D.; Mauk, A. G. *J. Am. Chem. Soc.* **1992**, *114*, 3619.

(53) Since the thiolate-bound species L-[4Fe–4S] is expected to be diamagnetic, detection and characterization of it in bulk solution will require the use of a spectroscopic method sensitive to the nature of L. Experiments are in progress using circular dichroism with optically active ligands and resonance Raman in order to determine whether such methods are suited to this task.

(54) More recent experiments, however, suggest that more extensive changes in cluster status may be involved. See: Haile, D. J.; Rouault, T. A.; Harford, J. B.; Kennedy, M. C,; Blondin, G. A.; Beinert, H.; Klausner, R. D. *Proc. Natl. Acad. Sci. U.S.A.* **1992**, *89*, 11735.